

The formation of the black hole in the X-ray binary system V404 Cyg

J.C.A. Miller-Jones,^{1,2*} P.G. Jonker,^{3,4} G. Nelemans,⁵ S. Portegies Zwart,^{6,7}
V. Dhawan,⁸ W. Briskin,⁸ E. Gallo,^{9,10} M.P. Rupen⁸

¹*NRAO Headquarters, 520 Edgemont Road, Charlottesville, VA, 22903, USA*

²*Jansky Fellow, National Radio Astronomy Observatory*

³*SRON, Netherlands Institute for Space Research, 3584 CA Utrecht, the Netherlands*

⁴*Harvard-Smithsonian Center for Astrophysics, Cambridge, MA 02138, USA*

⁵*Department of Astrophysics, IMAPP, Radboud University, Toernooiveld 1, 6525 ED, Nijmegen, the Netherlands*

⁶*Astronomical Institute ‘Anton Pannekoek’, University of Amsterdam, Kruislaan 403, 1098 SJ Amsterdam, the Netherlands*

⁷*Section Computational Science, University of Amsterdam, Kruislaan 403, 1098 SJ Amsterdam, the Netherlands*

⁸*NRAO, Array Operations Center, 1003 Lopezville Road, Socorro, NM 87801, U.S.A.*

⁹*Physics Department, Broida Hall, University of California, Santa Barbara, CA, 93106, USA*

¹⁰*Chandra Fellow*

Accepted 2008 December 15. Received 2008 December 11; in original form 2008 November 3

ABSTRACT

Using new and archival radio data, we have measured the proper motion of the black hole X-ray binary V404 Cyg to be $9.2 \pm 0.3 \text{ mas yr}^{-1}$. Combined with the systemic radial velocity from the literature, we derive the full three-dimensional heliocentric space velocity of the system, which we use to calculate a peculiar velocity in the range $47\text{--}102 \text{ km s}^{-1}$, with a best fitting value of 64 km s^{-1} . We consider possible explanations for the observed peculiar velocity, and find that the black hole cannot have formed via direct collapse. A natal supernova is required, in which either significant mass ($\sim 11M_{\odot}$) was lost, giving rise to a symmetric Blaauw kick of up to $\sim 65 \text{ km s}^{-1}$, or, more probably, asymmetries in the supernova led to an additional kick out of the orbital plane of the binary system. In the case of a purely symmetric kick, the black hole must have been formed with a mass $\sim 9M_{\odot}$, since when it has accreted $0.5\text{--}1.5 M_{\odot}$ from its companion.

Key words: X-rays: binaries – astrometry – radio continuum: stars – stars: individual (V404 Cyg) – stars: supernovae: general – stars: kinematics

1 INTRODUCTION

The proper motions of X-ray binary systems can be used to derive important information on the birthplaces and formation mechanisms of their compact objects. Since typical proper motions are of order a few milliarcseconds per year, high-resolution observations and long time baselines are required to measure the transverse motions of such systems across the sky. Proper motions have only been measured for a handful of X-ray binary systems to date (Mirabel et al. 2001, 2002; Ribó et al. 2002; Mirabel & Rodrigues 2003a,b; Dhawan et al. 2006, 2007), and only one X-ray binary, Sco X-1, has a measured proper motion, parallax distance, and radial velocity (Bradshaw et al. 1999; Cowley & Crampton 1975). With the position, proper motion, radial velocity,

and distance to the system, the full three-dimensional space velocity of the system can be derived. Along with system parameters such as the component masses, orbital period, donor temperature and luminosity, these parameters may be used to reconstruct the full evolutionary history of the binary system back to the time of compact object formation, as done for the systems GRO J1655-40 (Willems et al. 2005) and XTE J1118+480 (Fragos et al. 2007).

By studying the distribution of black hole X-ray binary velocities with compact object masses, we can derive constraints on theoretical models of black hole formation (e.g. Fryer & Kalogera 2001). The two most common theoretical scenarios for creating a black hole involve either a massive star collapsing directly into a black hole with very little or no mass ejection, or delayed formation in a supernova, as fallback onto the neutron star of material ejected during the explosion creates the black hole. In the latter case, con-

* email: jmiller@nrao.edu

straints on the magnitude and symmetry of any natal kick can also be derived. When the primary star reaches the end of its life and explodes as a supernova, the centre of mass of the ejected material continues to move with the velocity the progenitor had immediately before the explosion. The centre of mass of the binary system then recoils in the opposite direction. Such a kick (Blaauw 1961) is thus constrained to lie in the orbital plane. In addition, in the presence of asymmetries in the supernova explosion, a further, asymmetric, kick, which need not be in the orbital plane, may be imparted to the binary (see, e.g., Brandt & Podsiadlowski 1995; Portegies Zwart & Yungelson 1998; Lai et al. 2001, for more detailed overviews). While pulsar proper motions (Lyne & Lorimer 1994) and the high eccentricities of Be/X-ray binaries provide strong evidence for asymmetric kicks in neutron star formation (van den Heuvel & van Paradijs 1997; van den Heuvel et al. 2000), less attention has been paid to black hole binary systems. In two of the black hole X-ray binaries with some of the best observational constraints on the system parameters, XTE J1118+480 and GRO J1655-40, there is evidence for an asymmetric supernova kick (Gualandris et al. 2005; Willems et al. 2005). There is also some evidence suggesting an asymmetric kick in GRS 1915+105 (Dhawan et al. 2007), although in that case the uncertainty in the distance to the system precludes the derivation of strong constraints on the kick velocity. However, the black hole in Cygnus X-1 is inferred to have formed via direct collapse (Mirabel & Rodrigues 2003a). More black hole sources need to be studied to measure black hole kicks and investigate consequent formation mechanisms in order to constrain theoretical models of black hole formation.

1.1 V404 Cyg

V404 Cyg is a dynamically-confirmed black hole X-ray binary system, with a mass function of $6.08 \pm 0.06 M_{\odot}$ (Casares & Charles 1994). The system comprises a black hole accretor of mass $12^{+3}_{-2} M_{\odot}$ (Shahbaz et al. 1994) in a 6.5-d orbit with a $0.7^{+0.3}_{-0.2} M_{\odot}$ K0 IV stripped giant star (Casares et al. 1993; King 1993). The orbit is highly circular, with an eccentricity of $e < 3 \times 10^{-4}$, in agreement with the fact that tidal forces just before the onset of mass transfer should have recircularised the orbit following the supernova. Its low radial velocity ($-0.4 \pm 2.2 \text{ km s}^{-1}$; Casares & Charles 1994) has been taken as evidence for a small natal kick (Brandt et al. 1995; Nelemans et al. 1999).

In this paper we present measurements of the proper motion of V404 Cyg, and go on to derive its full three-dimensional space velocity, infer its Galactocentric orbit, and discuss the implications for the formation of the black hole in the light of the inferred natal kick from the supernova.

2 OBSERVATIONS AND DATA REDUCTION

In order to investigate the proper motion of the source, we interrogated the Very Large Array (VLA) archives for high-resolution observations of V404 Cyg. We selected only A-configuration observations at frequencies of 8.4 GHz and higher, to obtain the highest possible astrometric accuracy.

We further restricted the dataset to observations where the phase calibrator was J2025+3343, the phase reference source used in the High Sensitivity Array (HSA) observations of Miller-Jones et al. (2008). Since all positions are measured relative to the phase reference source, observations using a different secondary calibrator would potentially have been subject to a systematic positional offset.

The VLA data were reduced using standard procedures within the 31Dec08 version of AIPS (Greisen 2003). A script was written in PARSELTONGUE, the Python interface to AIPS, to automate the bulk of the calibration. We corrected the derived positions for shifts in the assumed calibrator position, using a reference position of $20^{\text{h}}25^{\text{m}}10^{\text{s}}.8421050$ $33^{\circ}43'00''.214430$ (J2000) for the calibrator source. All co-ordinates were precessed to J2000 values using the AIPS task UVFIX. Using data from the USNO (<http://maia.usno.navy.mil/ser7/finals2000A.all>), we corrected for offsets in (UT1-UTC), the difference between Universal Time (UT1) as set by the rotation of the Earth and measured by very long baseline interferometry (VLBI), and co-ordinated Universal Time (UTC), the atomic time (TAI) adjusted with leap seconds. Where measured offsets were available, we also corrected for shifts in antenna positions using the AIPS task VLANT. Source positions were measured by fitting an elliptical Gaussian to the source in the image plane, using the deconvolved, phase-referenced image prior to any self-calibration. The source was not resolved in any of the images. We added an extra positional uncertainty of 10 mas to the measured VLA positions, to account for systematic uncertainties in the astrometry. The list of observations and derived source positions is given in Table 1.

The dataset was enhanced by the use of two high-resolution VLBI measurements of the source position. We used the 8.4-GHz position of Miller-Jones et al. (2008), and also obtained a second measurement using global VLBI at 22 GHz, under proposal code GM064. Eight European stations (Cambridge, Effelsberg, Jodrell Bank MkII, Medicina, Metsahovi, Noto, Onsala, and Robledo), all ten Very Long Baseline Array (VLBA) stations, the phased VLA and the Green Bank Telescope (GBT) participated in the experiment. Data were taken from 21:30:00 UT on 2008 May 31 until 16:00:00 UT on 2008 June 1, with the European stations being on source for the first 12 h of the run (Robledo from 02:20:00 until 08:45:00 on 2008 June 1) and the North American stations for the second 12 h (Mauna Kea from 07:30:00, when the source rose in Hawaii). The overlap time, when both sets of stations were on source, was 5.5 h. The phase reference and fringe finder source was J2025+3343. We observed with a total bit rate of 512 Mb s^{-1} , with a bandwidth of 64 MHz per polarization. We observed in 150-s cycles, spending 1.5 min on the target and 1 min on the calibrator in each cycle. The VLA was phased up at the start of each calibrator scan, and we made referenced pointing observations with the larger dishes (the VLA, GBT, Effelsberg and Robledo) every 1–2 h. Data were reduced using standard procedures within AIPS. We detected the source at a significance level of 4.7σ .

Code	Date	MJD	Error (d)	Config.	Frequency (GHz)	RA	Error (sec)	Dec	Error (arcsec)
AH348	1990 Feb 16	47938.71	0.18	A	14.94	20 ^h 24 ^m 03 ^s .82854	0.00085	33° 52′ 02″.0348	0.0103
AH385	1990 Mar 08	47958.70	0.12	A	14.94	20 ^h 24 ^m 03 ^s .82896	0.00083	33° 52′ 02″.0379	0.0102
AH390	1990 Mar 25	47975.55	0.09	A	8.44	20 ^h 24 ^m 03 ^s .82865	0.00081	33° 52′ 02″.0439	0.0101
AH424	1991 Sep 25	48525.03	0.05	AB	14.94	20 ^h 24 ^m 03 ^s .82733	0.00276	33° 52′ 01″.9563	0.0235
AH424	1991 Sep 25	48525.04	0.05	AB	8.44	20 ^h 24 ^m 03 ^s .82321	0.00148	33° 52′ 02″.0143	0.0136
AH424	1992 Oct 20	48916.03	0.07	A	14.94	20 ^h 24 ^m 03 ^s .82752	0.00096	33° 52′ 02″.0208	0.0122
AH424	1992 Oct 20	48916.04	0.07	A	8.44	20 ^h 24 ^m 03 ^s .82673	0.00084	33° 52′ 02″.0196	0.0105
AH390	1993 Jan 28	49015.68	0.04	AB	14.94	20 ^h 24 ^m 03 ^s .82779	0.00222	33° 52′ 01″.9964	0.0173
AH390	1993 Jan 28	49015.68	0.02	AB	8.44	20 ^h 24 ^m 03 ^s .82427	0.00219	33° 52′ 02″.0317	0.0158
AH641	1998 May 04	50937.60	0.04	A	8.46	20 ^h 24 ^m 03 ^s .82493	0.00086	33° 52′ 01″.9820	0.0109
AH669	1999 Jul 04	51363.41	0.01	A	8.46	20 ^h 24 ^m 03 ^s .82479	0.00144	33° 52′ 01″.9721	0.0156
AH669	1999 Jul 13	51372.37	0.01	A	8.46	20 ^h 24 ^m 03 ^s .82431	0.00115	33° 52′ 01″.9984	0.0143
AH669	1999 Jul 26	51385.30	0.01	A	8.46	20 ^h 24 ^m 03 ^s .82508	0.00260	33° 52′ 01″.9470	0.0343
AH669	1999 Aug 22	51412.18	0.01	A	8.46	20 ^h 24 ^m 03 ^s .82443	0.00163	33° 52′ 01″.9429	0.0176
AH669	1999 Sep 01	51422.21	0.01	A	8.46	20 ^h 24 ^m 03 ^s .82417	0.00152	33° 52′ 02″.0063	0.0207
AH669	1999 Sep 04	51426.02	0.01	A	8.46	20 ^h 24 ^m 03 ^s .82397	0.00194	33° 52′ 01″.9464	0.0188
AH669	2000 Oct 20	51837.33	0.01	A	8.46	20 ^h 24 ^m 03 ^s .82718	0.00595	33° 52′ 01″.9676	0.0405
AR476	2002 Feb 03	52308.69	0.01	A	8.46	20 ^h 24 ^m 03 ^s .82325	0.00088	33° 52′ 01″.9481	0.0108
AR476	2002 Mar 01	52334.54	0.01	A	8.46	20 ^h 24 ^m 03 ^s .82586	0.00257	33° 52′ 01″.9457	0.0224
AH823	2003 Jul 29	52849.30	0.29	A	8.46	20 ^h 24 ^m 03 ^s .82440	0.00101	33° 52′ 01″.9317	0.0120
BG168	2007 Dec 02	54436.84	0.09	HSA	8.42	20 ^h 24 ^m 03 ^s .82129	0.000010	33° 52′ 01″.8993	0.0003
GM064	2008 May 31	54618.42	0.25	Global	22.22	20 ^h 24 ^m 03 ^s .821082	0.000009	33° 52′ 01″.8957	0.0001

Table 1. Summary of the VLA and VLBI observations. The errors on the MJD values are taken as half the length of the observation. The quoted positional errors for the VLA observations are the sum in quadrature of the statistical errors and a systematic uncertainty of 10 mas. All co-ordinates are for epoch J2000. The coordinate system is based on the assumed position of the calibrator source J 2025+3343, taken to be (J 2000) 20^h25^m10^s.8421050(224) 33° 43′ 00″.21443(42). The HSA and global VLBI observations have been corrected for parallax, assuming a source distance of 4 kpc, and accounting for the uncertainty in the parallax when calculating the positional error bars.

3 RESULTS

Fig. 1 shows the measured Right Ascension and Declination as a function of time, over the ~ 20 years since the 1989 outburst of V404 Cyg. The best fitting proper motions, in Right Ascension and Declination respectively, are

$$\mu_{\alpha} \cos \delta = -4.99 \pm 0.19 \text{ mas y}^{-1} \quad (1)$$

$$\mu_{\delta} = -7.76 \pm 0.21 \text{ mas y}^{-1}. \quad (2)$$

Thus the total proper motion is $\mu = 9.2 \pm 0.3 \text{ mas y}^{-1}$. All uncertainties are 68 per cent confidence limits, and unless otherwise noted we will henceforth quote 1σ error bars on all measurements.

The fit gives a reference position (prior to correcting for the effects of the unknown parallax) of 20^h24^m03^s.82177(2) 33° 52′ 01″.9088(3) (J 2000) on MJD 54000.0, from which we can use the proper motion to determine the predicted position at any future time.

3.1 Converting to Galactic Space Velocity co-ordinates

With the systemic radial velocity of $-0.4 \pm 2.2 \text{ km s}^{-1}$ measured from optical H α studies (Casares & Charles 1994), we can calculate, for a given source distance, the full three-dimensional space velocity of the system. The best constraint on the source distance is $4.0_{-1.2}^{+2.0} \text{ kpc}$ (Jonker & Nelemans 2004). Using the transformations of Johnson & Soderblom (1987), and the standard solar motion of ($U_{\odot} = 10.0 \pm 0.36$, $V_{\odot} = 5.25 \pm 0.62$, $W_{\odot} = 7.17 \pm 0.38$) km s^{-1} (Dehnen & Binney 1998), we can compute the heliocentric Galactic space velocity components U , V and W (defined as U positive towards the Galactic Centre, V positive towards $l = 90^{\circ}$, and W positive towards the

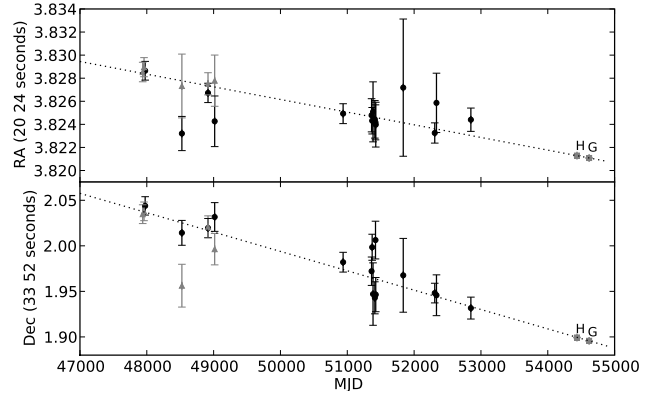


Figure 1. Top panel: Measured Right Ascension as a function of time, from 1990 to 2007. Bottom panel: Declination as a function of time. The dotted lines are the best fitting proper motions, $\mu_{\alpha} = (-4.99 \pm 0.19) \times 10^{-4} \text{ sec y}^{-1}$ in R.A. and $\mu_{\delta} = (-7.76 \pm 0.21) \text{ mas y}^{-1}$ in Dec.. The black dots are the VLA 8.4 GHz points and the light grey triangles are the 15-GHz VLA measurements. The dark grey squares labelled ‘H’ and ‘G’ are from the 8.4-GHz HSA observations of Miller-Jones et al. (2008) and the 22-GHz global VLBI observations reported in this paper, respectively.

North Galactic Pole). The derived system parameters are given in Table 2.

For a given distance, the expected values of U and V can be calculated, assuming the source participates in the Galactic rotation. Reid & Brunthaler (2004) determined the angular rotation rate of the LSR at the Sun, $\Theta_0/R_0 = 29.45 \pm 0.15 \text{ km s}^{-1} \text{ kpc}^{-1}$. Assuming a Galactocentric distance of 8.0 kpc (Reid 1993), this implies a circular velocity of 236 km s^{-1} . For circular rotation about the Galactic Centre, the W component of the velocity is expected to be

Parameter	Value
Galactic longitude l	73.12°
Galactic latitude b	-2.09°
Distance d (kpc)	$4.0^{+2.0}_{-1.2}$
Systemic velocity γ (km s^{-1})	-0.4 ± 2.2
Proper motion $\mu_\alpha \cos \delta$ (mas y^{-1})	-4.99 ± 0.19
Proper motion μ_δ (mas y^{-1})	-7.76 ± 0.21
U (km s^{-1})	$177.1 \pm 3.8^{+83.7}_{-50.2}$
V (km s^{-1})	$-46.1 \pm 2.4^{+15.3}_{-25.5}$
W (km s^{-1})	$0.2 \pm 3.7^{+2.1}_{-3.5}$
$U - \langle U \rangle$ (km s^{-1})	$62.0^{+39.4}_{-17.4}$
$V - \langle V \rangle$ (km s^{-1})	$-16.1^{+6.5}_{-0.0}$
$W - \langle W \rangle$ (km s^{-1})	$0.2^{+2.1}_{-3.5}$
v_{pec} (km s^{-1})	$64.1 \pm 3.7^{+37.8}_{-16.6}$

Table 2. Measured and derived parameters. U , V and W are the Galactic space velocity components in the direction of the Galactic Centre, $l = 90^\circ$ and $b = 90^\circ$ respectively. The first set of error bars accounts for uncertainties in the measured space velocities only, and the second takes into account the distance uncertainty. $U - \langle U \rangle$, $V - \langle V \rangle$ and $W - \langle W \rangle$ are the discrepancies from the velocities that would be expected for Galactic rotation. Summing these discrepancies in quadrature gives the peculiar velocity, v_{pec} . The major source of error in these values is the distance uncertainty.

zero. As done by Dhawan et al. (2007) for GRS 1915+105, we can transform the measured values of U and V into radial and circular velocities about the Galactic Centre, expected to be $v_{\text{rad}} = 0 \text{ km s}^{-1}$ and $v_{\text{circ}} = 236 \text{ km s}^{-1}$ respectively. Fig. 2 shows the derived radial, circular and W velocities and the peculiar velocity of V404 Cyg. The peculiar velocity is defined to be the difference between the measured 3-dimensional space velocity and that expected for a source participating in the Galactic rotation,

$$v_{\text{pec}} = (v_{\text{rad}}^2 + (v_{\text{circ}} - 236)^2 + W^2)^{1/2} \quad (3)$$

For the range of distances found by Jonker & Nelemans (2004), 2.8–6.0 kpc, it is clear that the peculiar velocity is non-zero. We derive a value of $v_{\text{pec}} = 64.1 \pm 3.7^{+37.8}_{-16.6} \text{ km s}^{-1}$, where the first error bar accounts for statistical error in the space velocities, and the second for the distance uncertainty. The predominant component of the peculiar velocity is radial, with a circular velocity slightly faster than expected, and a velocity out of the Galactic plane consistent with zero.

4 THE ORBITAL TRAJECTORY IN THE GALACTIC POTENTIAL

From the known source position and the measured spatial velocity components, we can integrate backwards in time to compute the orbital trajectory of the system in the potential of the Galaxy. Using a fifth-order Runge-Kutta algorithm (Press et al. 1992) to perform the integration, we compared the predictions of several different models for the Galactic potential (Carlberg & Innanen 1987, using the revised parameters of Kuijken & Gilmore 1989; Paczyński 1990; Johnston et al. 1995; Wolfire et al. 1995; Flynn et al. 1996; de Oliveira et al. 2002), all using some combination of one or more disc, spherical bulge and halo components.

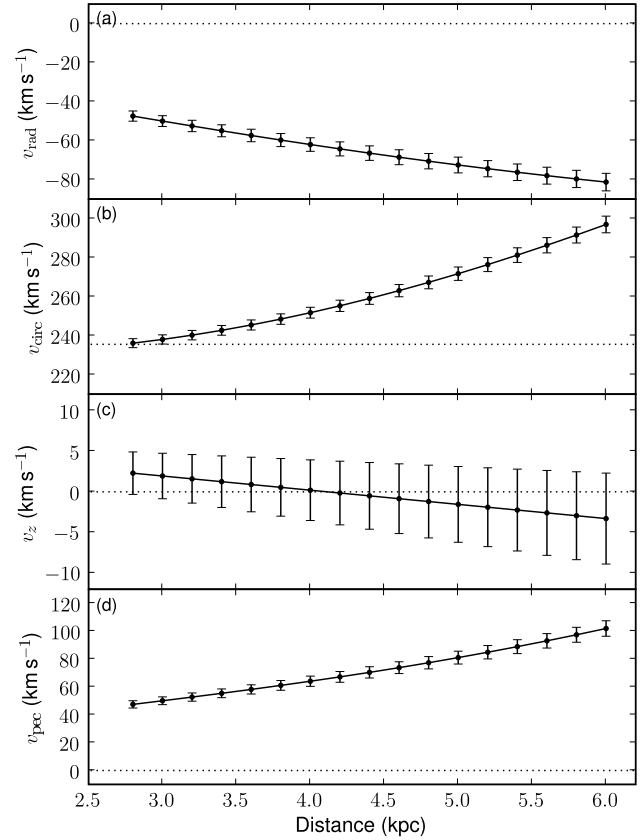


Figure 2. Derived Galactocentric velocities of V404 Cyg, as a function of source distance. (a) shows the radial velocity, v_{rad} , (b) shows the circular velocity, v_{circ} , (c) shows the velocity out of the Galactic plane, W , and (d) shows the peculiar velocity, v_{pec} , i.e. the difference from the values expected for a source participating in the Galactic rotation. Dotted lines show the expected values of 0 km s^{-1} for the radial, W and peculiar velocities, and 236 km s^{-1} for the circular velocity. Error bars only account for uncertainties in the space velocity components, assuming zero error on the distance at each plotted point.

A representative orbit reconstruction using the model of Johnston et al. (1995) is shown in Fig. 3. While the errors in the space velocity components make little difference to the computed orbital trajectory for a given model, the uncertainty in the distance has much more of an effect. Fig. 4 compares the trajectories computed for 2.8, 4.0 and 6.0 kpc, the lower, mean and upper bounds to the possible range of distances. A larger source distance implies a more elliptical orbit, which reaches further from the Galactic Centre at apogalacticon.

Comparing the different models for the Galactic potential, we find that the predicted orbital trajectories in the Galactic plane begin to diverge significantly after only 25–30 Myr. In the perpendicular direction, the predictions diverge even faster, within 2–3 Myr. Given the uncertainty in the source distance and Galactic potential, it is clearly impossible to integrate back in time over 0.4–0.8 Gyr (Section 5) to locate the birthplace of the system. However, for a given source distance, we can average over the ensemble of model predictions to derive some generic properties of the orbit. The eccentricity e , semi-major axis a , and the dis-

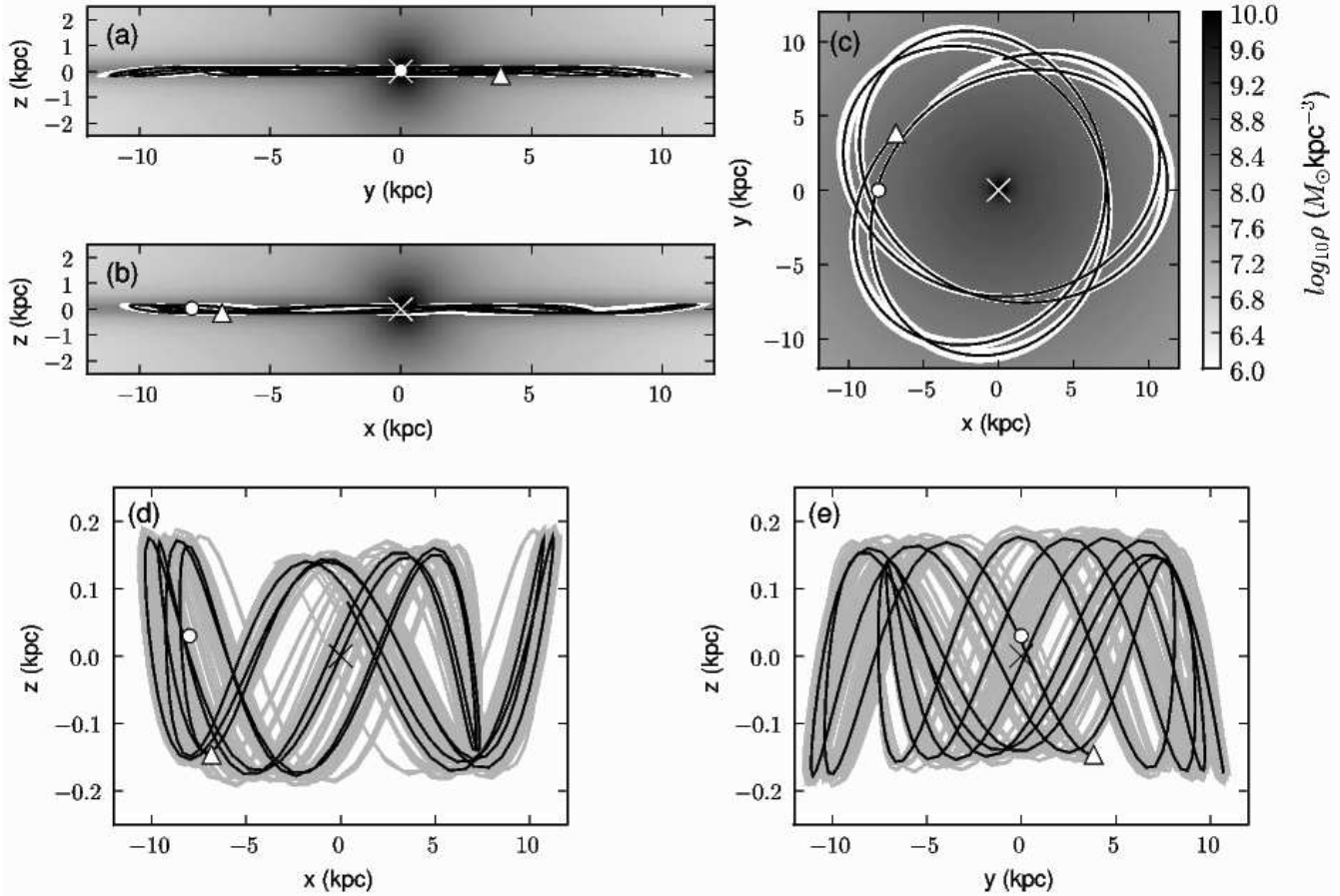


Figure 3. The computed orbit of V404 Cyg over the last 1 Gyr, using the Galactic potential of Johnston et al. (1995) and assuming a current source distance of 4.0 kpc. In (a), (b) and (c), the greyscale is a logarithmic representation of the Galactic mass density ($M_{\odot} \text{ kpc}^{-3}$), the black line denotes the computed orbit for the best fitting space velocities and positions, and the white trace indicates the error due to uncertainty in the space velocity components. For clarity, the effect of the distance uncertainty is not shown (see Fig. 4). Panels (d) and (e) are a zoomed-in version of the x - z and y - z planes respectively (x , y and z defined as the directions $l = 0^{\circ}$, $l = 90^{\circ}$, $b = 90^{\circ}$ respectively), with the black line indicating the best-fitting trajectory and the grey trace once again indicating the spread due to uncertainty in the measured space velocities only. In all panels, the cross marks the Galactic Centre, and the open circle and triangle mark the current positions of the Sun and V404 Cyg respectively.

tances of the apsides, r_{\max} and r_{\min} , for the motion in the Galactic plane, the maximum height reached above or below the plane, z_{\max} , and the minimum and maximum values of the peculiar velocity, $v_{\text{pec},\min}$ and $v_{\text{pec},\max}$, are given in Table 3.

We can compare these values with those of the thick and thin disk populations. Binney & Merrifield (1998) give the velocity dispersions in the radial, azimuthal and vertical directions (relative to the Galactic plane) for both stellar populations, based on the data of Edvardsson et al. (1993), for stars within 80 pc of the Sun. A set of Monte Carlo simulations established that the typical planar eccentricities of the thin and thick disk populations were 0.12 ± 0.06 and 0.29 ± 0.15 respectively, while the typical maximum height reached above the plane was 0.17 ± 0.14 and 0.56 ± 0.61 kpc respectively. Unless V404 Cyg is at the maximum possible distance, it is likely to have originated as a member of the thin disk population (as also suggested by the age, metallic-

ity and component masses of the system), and received some sort of kick which increased the planar eccentricity and the component of velocity out of the Galactic plane.

5 THE PECULIAR VELOCITY

The current peculiar velocity of the system is $64.1 \pm 3.7^{+37.8}_{-16.6} \text{ km s}^{-1}$. However, owing to its orbit in the Galactic potential, this is not a conserved quantity. For a distance of 4 kpc, we find that the peculiar velocity varies between 39 and 79 km s^{-1} (see Table 3 and Fig. 5). We go on to examine potential explanations for this peculiar velocity.

5.1 Symmetric supernova kick

If it formed with a natal supernova, the system can receive a Blaauw kick (Blaauw 1961), whereby the binary recoils to

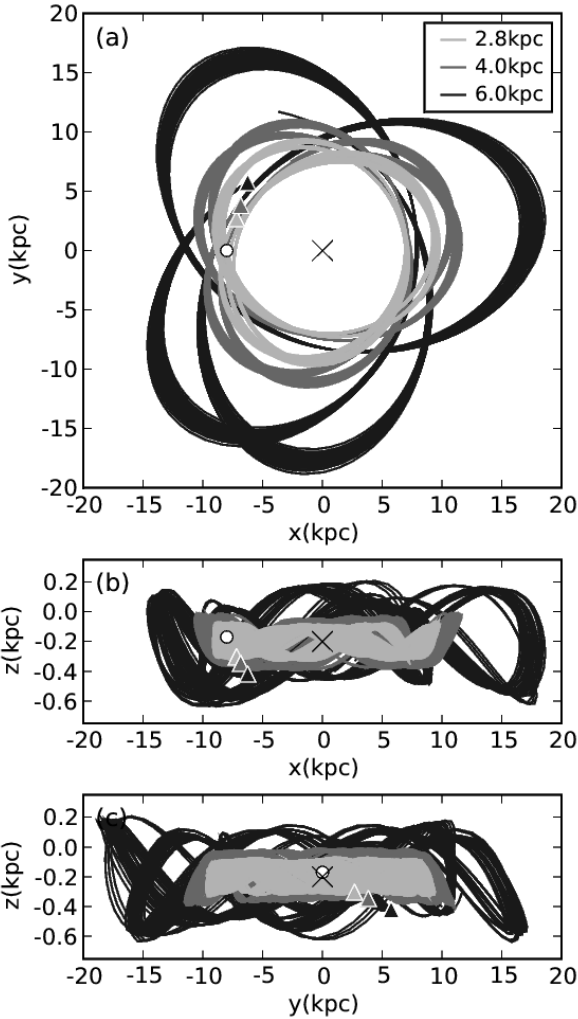


Figure 4. The effect of the distance uncertainty on the computed Galactocentric orbit of V404 Cyg. Trajectories have been computed for the minimum, best fitting and maximum distances derived by Jonker & Nelemans (2004), using the measured space velocities and the Galactic potential of Johnston et al. (1995). For each distance, the spread in the trajectories due to uncertainties in the space velocity components has been plotted. In all panels, the cross marks the Galactic Centre, and the open circle and triangles mark the current positions of the Sun and V404 Cyg (at its different distances) respectively.

conserve momentum after mass is instantaneously ejected from the primary. For the binary to remain bound after the supernova, the ejected mass ΔM must be less than half the total mass of the system. A maximum ejected mass translates to a maximum recoil velocity of the binary, for which an expression was derived by Nelemans et al. (1999),

$$v_{\max} = 213 \left(\frac{\Delta M}{M_{\odot}} \right) \left(\frac{m}{M_{\odot}} \right) \left(\frac{P_{\text{re-circ}}}{\text{d}} \right)^{-1/3} \times \left(\frac{M_{\text{BH}} + m}{M_{\odot}} \right)^{-5/3} \text{ km s}^{-1}, \quad (4)$$

where M_{BH} and m are the masses of the black hole and the secondary immediately after the supernova, before mass transfer has begun, and $P_{\text{re-circ}}$ is the period of the orbit once it has recircularized following the supernova, re-

Distance	2.8 kpc	4.0 kpc	6.0 kpc
r_{\max} (kpc)	9.8 ± 0.4	11.7 ± 0.7	20.2 ± 4.4
r_{\min} (kpc)	7.0 ± 0.1	7.2 ± 0.1	7.9 ± 0.1
z_{\max} (kpc)	0.13 ± 0.02	0.20 ± 0.03	0.47 ± 0.14
a (kpc)	8.4 ± 0.2	9.4 ± 0.4	14.1 ± 2.2
e	0.16 ± 0.02	0.24 ± 0.03	0.42 ± 0.07
$v_{\text{pec,min}}$ (km s^{-1})	21.9 ± 5.1	38.9 ± 6.4	82.4 ± 7.4
$v_{\text{pec,max}}$ (km s^{-1})	56.5 ± 4.9	78.8 ± 5.7	134.3 ± 10.3

Table 3. Derived parameters of the Galactocentric orbit, averaged over the ensemble of models for the Galactic potential. The parameters are the maximum and minimum distances from the Galactic Centre measured in the plane (r_{\max} and r_{\min}), the maximum distance reached above or below the plane (z_{\max}), the semi-major axis a , the orbital eccentricity e (both calculated in the plane), and the minimum and maximum peculiar velocity ($v_{\text{pec,min}}$ and $v_{\text{pec,max}}$ respectively). Uncertainties are the scatter due to both the errors on the measured velocities and the differing models for the Galactic Potential.

lated to the orbital period immediately after the supernova has occurred by $P_{\text{re-circ}} = P_{\text{post-SN}}(1 - e_{\text{post-SN}}^2)^{3/2}$. Recircularization occurs before the start of mass transfer from the secondary to the black hole, due to the strong tidal forces present once the secondary has evolved and expanded sufficiently to come close to filling its Roche Lobe.

During its X-ray binary phase, the system undergoes mass transfer from the donor star to the black hole, increasing the black hole mass and orbital period and reducing the donor mass. In the case of conservative mass transfer, angular momentum conservation and Kepler's Third Law imply that these parameters evolve as

$$P \propto (M_{\text{BH}}m)^{-3}. \quad (5)$$

While we have no exact constraint on how long ago mass transfer began, we can use the current orbital period and component masses (Shahbaz et al. 1994) together with Equation 5 to find the system parameters at any point in the past, and the implied maximum ejected mass and recoil velocity of a supernova which would have created a system with those parameters (from Equation 4). This is shown in Fig. 6 for three possible current configurations of donor and accretor mass.

As mass is transferred from donor to accretor, the orbital period increases (Equation 5). Thus for a larger transferred mass, M_{trans} , (a smaller initial black hole mass and a less recent onset of mass transfer) the orbital period at the onset of mass transfer is smaller. The pre-supernova orbital period, which is smaller due to the mass loss in the explosion (middle line in the top left hand panel of Fig. 6), cannot be so short that either the black hole progenitor or its companion fills its Roche lobe, setting a minimum possible pre-supernova orbital period (lower line in the top left hand panel of Fig. 6). For small values of M_{trans} , the maximum mass lost in the supernova is equal to half the total system mass, and the maximum kick velocity v_{\max} increases via Equation 4 because both the post-supernova donor mass increases and the post-supernova period decreases with increasing M_{trans} . Where the period constraint becomes important, the maximum mass lost in the supernova decreases, being set by the shortest allowed pre-supernova orbital pe-

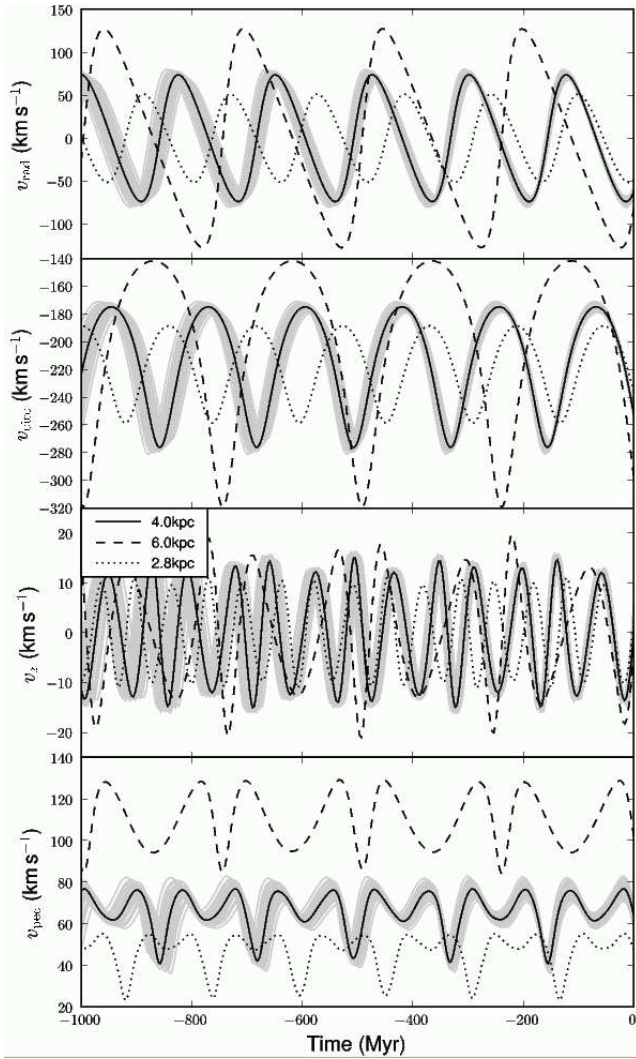


Figure 5. Variation in Galactocentric radial velocity v_{rad} , circular velocity v_{circ} , perpendicular velocity v_z , and peculiar velocity v_{pec} , as a function of time while integrating the orbit backwards over the last Gyr, using the potential of Johnston et al. (1995). Solid, dotted and dashed lines are for source distances of 4.0, 2.8 and 6.0 kpc respectively. The grey lines show the uncertainty arising from the error bars on the measured space velocities, for a distance of 4.0 kpc. The peculiar velocity varies as a function of time.

riod. The decreasing mass loss in the explosion then offsets the increasing post-supernova donor mass, and the maximum possible kick velocity decreases as M_{trans} increases further.

Equation 5 is valid only for the case of conservative mass transfer. However, there are strong indications that this assumption is not valid for V404 Cyg. At the very least, the radio outbursts (e.g. Han & Hjellming 1992) suggest that material is being lost to jet outflows. Podsiadlowski et al. (2003) calculated binary evolution tracks for a $10M_{\odot}$ black hole in orbit with donors of mass 2– $17M_{\odot}$ (for there to have been any symmetric kick, Fig. 6 shows that the transferred mass must be $< 2.5M_{\odot}$, implying that the initial secondary must have been less massive than $\sim 3.5M_{\odot}$), some of which they found could reproduce the system param-

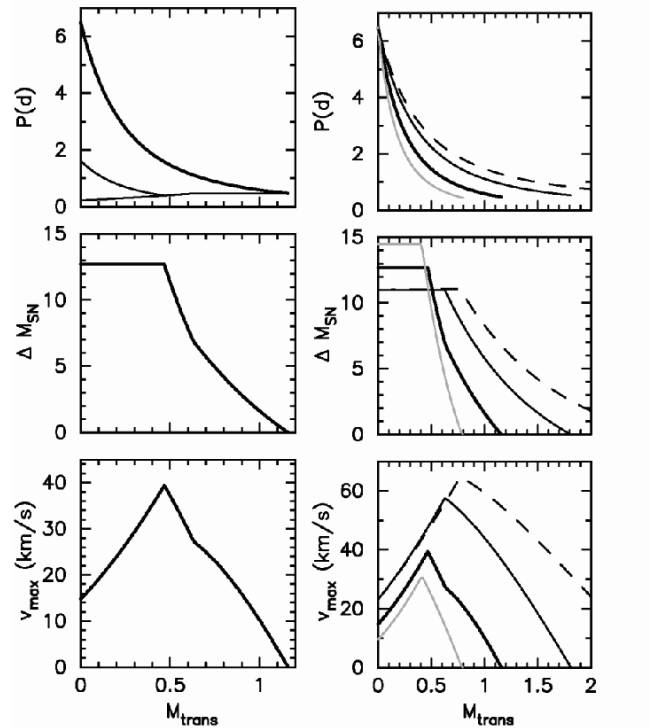


Figure 6. Evolution of the post-supernova binary orbital period (top panels), maximum possible mass ejected in the supernova (middle panels), and maximum possible velocity kick (lower panels), as a function of total mass transferred since the supernova from the secondary to the black hole. Left-hand panels are all for the case of conservative mass transfer, for current component masses of $(M_{\text{BH}}, m) = (12, 0.7) M_{\odot}$. The top left plot shows the post-supernova orbital period (thick solid line), the pre-supernova orbital period (middle line) and the minimum permitted pre-supernova orbital period in which neither the helium star progenitor nor the main sequence companion fills its Roche lobe (bottom line). The right-hand panels show the situation for conservative mass transfer using different current component masses, and one case of non-conservative mass transfer. Thick solid lines are for current component masses of $(M_{\text{BH}}, m) = (12, 0.7) M_{\odot}$, thin solid lines are for $(10, 1) M_{\odot}$ and grey lines are for $(14, 0.5) M_{\odot}$, assuming conservative mass transfer in all cases. Dashed lines indicate non-conservative mass transfer for the $(10, 1) M_{\odot}$ case, with ten per cent of the mass transferred being lost from the system.

eters of V404 Cyg extremely well. They took into account non-conservative mass transfer, whereby mass transferred in excess of the Eddington rate is lost from the system. A comparison with the equations for conservative mass transfer suggested that the orbital period increases more slowly in the non-conservative case, by a factor of at most 2. As an example of how this could affect the maximum Blaauw kick velocity, the dashed lines in Fig. 6 are for the current case of a $10M_{\odot}$ accretor with a $1M_{\odot}$ donor, with 10 per cent of the transferred mass being lost from the system and the orbital period increasing a factor 2 more slowly than predicted by Equation 5.

Our calculations show that for V404 Cyg, it is just possible to achieve a kick of 64 km s^{-1} using only symmetric mass loss in the supernova (a Blaauw kick). If the explosion occurred at a point in the Galactocentric orbit where

the peculiar velocity was minimized (Fig. 5), this could be sufficient to explain the observed peculiar velocity, particularly if the system is towards the lower end of the possible range of distances. However, to achieve such a large kick requires fine-tuning the parameters, to give a relatively low initial black hole mass (closer to $9.2M_{\odot}$ than the best fitting value of $12M_{\odot}$) and an ejection of $\sim 11M_{\odot}$ during the supernova. Such a large mass loss, in combination with the system parameters (a $\sim 9M_{\odot}$ black hole with a low-mass donor), do not make this scenario very plausible (see, e.g., Fryer & Kalogera 2001, for theoretical estimates of the amount of mass ejected in a supernova as a function of progenitor mass; to form a $9M_{\odot}$ black hole requires a progenitor of $25\text{--}30M_{\odot}$, in which case the mass ejected in the supernova is expected to be $< 3M_{\odot}$). We find it unlikely that a symmetric kick alone is sufficient to explain the observed peculiar velocity.

5.2 Velocity dispersion in the disc

The donor star in V404 Cyg is a K0 subgiant (Casares & Charles 1994) of mass $0.7^{+0.3}_{-0.2}M_{\odot}$ (Shahbaz et al. 1994). King (1993) demonstrated that the system is a stripped giant, which evolves on the nuclear timescale of the donor star, which is in the range 0.4–0.8 Gyr. Thus the secondary was initially significantly more massive, and has transferred mass to the black hole. From Fig. 6, the donor star is unlikely to have transferred more than $2.5M_{\odot}$ to the black hole during the mass transfer phase, implying an initial donor mass of $< 3.5M_{\odot}$. The evolutionary tracks of Podsiadlowski et al. (2003) show that such a system would take of order 0.7–0.8 Gyr to evolve to an orbital period of 6.5 d, in agreement with the range given by King (1993). In 0.8 Gyr, the system has made 3.5–5 orbits in the potential of the Galaxy (depending on the model used for the Galactic potential; see Section 4), so could well have received some component of peculiar velocity in the Galactic plane owing to non-axisymmetric forces such as scattering from the potentials of spiral arms or interstellar cloud complexes (Wielen 1977). However, estimates of the velocity dispersion of the thin disk population (Dehnen & Binney 1998; Mignard 2000) show that for F0–F5 stars (with initial masses comparable to that estimated for the donor star in V404 Cyg prior to the onset of mass transfer), it is of order 28 km s^{-1} .

Mignard (2000) fitted the Sun’s peculiar motion and the differential velocity field caused by the Galactic rotation to the parallaxes and proper motions measured by Hipparcos. Examining the fit residuals showed the peculiar velocities to follow a three-dimensional Gaussian distribution, with the predicted scatter in the velocity in Galactic longitude being given by $(0.7 < u^2 >)^{1/2}$, where $< u^2 >$ is the velocity dispersion in the radial direction, determined as $< u^2 >^{1/2} = 22.5 \pm 0.3\text{ km s}^{-1}$ for F0–F5 stars. The measured peculiar velocity of V404 Cyg in the longitudinal direction is $-64.0^{+18.5}_{-37.7}\text{ km s}^{-1}$, implying a probability of 7×10^{-4} of being caused by Galactic velocity diffusion if the source is at 4 kpc, and only 1.6×10^{-2} even if the source is at 2.8 kpc. Thus this mechanism is unlikely to account for the observed and inferred range of peculiar velocities.

5.3 An asymmetric supernova kick?

If neither the effects of stellar diffusion nor a symmetric kick can explain the observed peculiar velocity, it could instead be the effect of an asymmetric kick during the supernova. The smaller dispersion in z -distance (distance above or below the Galactic plane) of black hole X-ray binaries when compared to neutron star systems had been interpreted as evidence for smaller kicks when forming black holes (White & van Paradijs 1996). However, Jonker & Nelemans (2004), using a larger sample and revised distance estimates for the sources, found no evidence for such a discrepancy, suggesting that black holes can receive natal kicks comparable with those seen in neutron star systems. Recent analysis of the space velocities of the black hole X-ray binaries XTE J1118+480 (Gualandris et al. 2005) and GRO J1655-40 (Willems et al. 2005) found evidence for asymmetric kicks in these two systems, with such a kick being mandated in the case of XTE J1118+480 (Fragos et al. 2007).

An asymmetric kick is not constrained to lie in the orbital plane, as in the case of a Blaauw kick. While the inclination angle of the system to the line of sight is well-constrained to be $56^{\circ} \pm 4^{\circ}$ (Shahbaz et al. 1994), the longitude of the ascending node, Ω , with respect to the sky plane is not known, so we cannot determine the absolute orientation of the binary orbital plane. However, for a given value of Ω , we can determine the orientation of the orbital plane with respect to the Galactic axes x , y and z (corresponding to the velocity components U , V and W). We assume that the orientation of the orbital plane does not change with time. For any point during its Galactocentric orbit, we can use the positions and velocities computed in Section 4 to calculate the component of the peculiar motion perpendicular to the orbital plane, v_{\perp} , which provides a lower limit to the asymmetric kick velocity should the supernova have occurred at that point in time. Assuming all values $0 < \Omega < 2\pi$ are equally likely, we can run Monte Carlo simulations to find the probability that the component of the peculiar velocity perpendicular to the orbital plane is equal to or less than would be expected for the progenitor from the typical velocity dispersion of massive stars (taken as 10 km s^{-1} in one component; see Mignard 2000). Fig. 7 shows the probability that v_{\perp} is less than 10 km s^{-1} for the mean and extreme values of the distance, as a function of time. The probability is low, of order 10–20 per cent, with little variation in the mean probability as a function of source distance. It is therefore unlikely (although possible, except for certain short periods of time) that the measured peculiar velocity perpendicular to the binary orbital plane can be attributed to the velocity dispersion of the system prior to the supernova. Since a symmetric kick cannot give rise to velocity out of the orbital plane, it is probable that there was an asymmetric kick during the formation of the black hole.

6 DISCUSSION

It appears that a supernova is required to explain the peculiar velocity of V404 Cyg. Thus the black hole in this system did not form via direct collapse. From the range of peculiar velocities inferred during the Galactocentric orbit of the system, a symmetric supernova kick could just be sufficient to

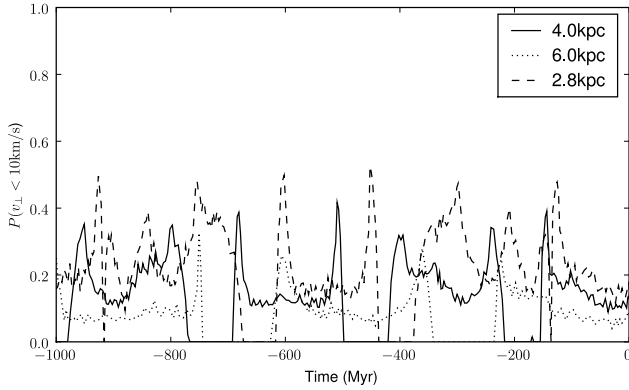


Figure 7. Probability that the component of the peculiar velocity perpendicular to the orbital plane is less than 10 km s^{-1} . We assumed a uniform probability for the longitude of the ascending node, for angles in the range $0 < \Omega < 2\pi$, and derived the probabilities for the best-fitting distance (4.0 kpc; solid line), and the upper (6.0 kpc; dotted line) and lower (2.8 kpc; dashed line) limits to the distance. A low probability implies that it is likely that the velocity perpendicular to the orbital plane is high, so the system has received an asymmetric kick at formation.

explain the observations if the source is at the lower end of the allowed range of distances. However, the mass loss required, as well as the component of peculiar velocity inferred to lie perpendicular to the orbital plane, make it likely that the system was subject to an asymmetric kick during black hole formation.

The full three-dimensional space velocities have been measured for a handful of other black hole systems. XTE J1118+480 (Mirabel et al. 2001) and GRO J1655-40 (Mirabel et al. 2002) are both in highly eccentric orbits around the Galactic Centre. An asymmetric natal kick is required for XTE J1118+480 (Fragos et al. 2007), and believed to have been likely in GRO J1655-40 (Willems et al. 2005). The high-mass X-ray binary Cygnus X-1 (Mirabel & Rodrigues 2003a) is moving at only $9 \pm 2 \text{ km s}^{-1}$ with respect to its parent association Cyg OB3, implying that $< 1 M_{\odot}$ was ejected in the natal supernova, and that the black hole formed by direct collapse. GRS 1915+105 on the other hand, has been inferred to have an orbit and peculiar velocity (Dhawan et al. 2007) fairly similar to that of V404 Cyg. Dhawan et al. (2007), using a Galactocentric distance of $R_0 = 8.5 \text{ kpc}$ and a circular velocity of $\Theta_0 = 220 \text{ km s}^{-1}$ for the LSR, found that a symmetric supernova kick and stellar diffusion were insufficient to explain the peculiar velocity unless the source was located at 9–10 kpc, where the peculiar velocity is minimized. However, using the values of $R_0 = 8.0 \text{ kpc}$ and $\Theta_0 = 236 \text{ km s}^{-1}$ assumed in this paper gives a minimum peculiar velocity of 23 km s^{-1} for a source distance of 10 kpc, which could then in principle be explained by a symmetric supernova explosion or stellar diffusion. While a distance at the lower end of the allowed range would give a higher value for the current peculiar velocity, the peculiar velocity would still be sufficiently low at certain points in the Galactocentric orbit for an asymmetric kick not to be required. However, if the source is at the upper end of the possible distance range ($\gtrsim 12 \text{ kpc}$), the peculiar velocity is high enough throughout the orbit that an asymmetric kick becomes necessary.

Without knowing the source distance, we cannot definitively determine its formation mechanism. We also note that the momentum imparted by a kick of 23 km s^{-1} to such a $14 M_{\odot}$ black hole (Greiner et al. 2001) is similar to that gained by a neutron star receiving a kick of a few hundred km s^{-1} (e.g. Lyne & Lorimer 1994; Hansen & Phinney 1997), so owing to its large mass, even such a low peculiar velocity for GRS 1915+105 would not necessarily rule out a natal kick.

For V404 Cyg, the derived components of the system velocity in the Galactic plane, U and V , are much larger than W , the velocity out of the plane (Table 2). While this is to be expected since the Galactic rotation of 236 km s^{-1} forms a component of both U and V , but not W , accounting for the Galactic rotation (giving the $U - \langle U \rangle$ and $V - \langle V \rangle$ terms in Table 2) does not remove this discrepancy between the components of the peculiar velocity in and out of the plane. A similar discrepancy is observed for the other four black hole systems with measured three-dimensional space velocities (Mirabel et al. 2001, 2002; Mirabel & Rodrigues 2003a; Dhawan et al. 2007), even accounting for the ranges of values allowed by the uncertainties in the system parameters. However, as shown in Fig. 5, the velocity components change with time, so we reconstructed the Galactocentric orbits of all five sources. This showed that the W component of velocity can be significantly greater than the peculiar velocity in the plane for XTE J1118+480, and can be of a similar magnitude to the component in the plane at certain points in the orbits of Cygnus X-1 and GRS 1915+105. With only five systems, we are dealing with small number statistics, but these results are consistent with there being no preferred orientation of the peculiar velocity relative to the Galactic plane. Indeed, considering the known population of black hole X-ray binaries, including those with no measured space velocity, the distribution in z (Jonker & Nelemans 2004) demonstrates that a number of systems must have a significant W velocity at certain points in their orbits, in order to reach the distances of several hundred parsecs above or below the plane at which they are currently observed. Thus there is no observational evidence to suggest that the natal kick distribution should not be isotropic.

Thus the two systems with the lowest black hole masses, XTE J1118+480 and GRO J1655-40 (both of order $6\text{--}7 M_{\odot}$ Orosz 2003), are found to have required asymmetric kicks during the formation of the black hole. For the higher-mass systems, the situation is less clear-cut. Cygnus X-1, V404 Cyg and GRS 1915+105 all have masses of $> 10 M_{\odot}$. While Cygnus X-1 appears to have formed by direct collapse, the peculiar velocity of V404 Cyg implies that a supernova must have occurred, and an asymmetric kick seems likely to have been required in this system, contrary to assertions that black holes of $10 M_{\odot}$ form by direct collapse (e.g. Mirabel 2008). For GRS 1915+105, we cannot definitively determine its formation mechanism without an accurate distance to the source. Regardless, with only five systems, no clear trends with black hole mass can be identified. In order to better constrain the formation mechanisms of stellar-mass black holes, the space velocities of more such systems with a range of black hole masses need to be measured, to constrain the frequency of occurrence of natal kicks, and hence supernova explosions.

7 CONCLUSIONS

We have measured the proper motion of V404 Cyg using 20 years' worth of VLA and VLBI radio observations. Together with the radial velocity and constraints on the distance of the system, this translates to a peculiar motion of $64.1 \pm 3.7^{+37.8}_{-16.6} \text{ km s}^{-1}$. Given the measured proper motion, the black hole cannot have been formed via direct collapse. A supernova is required to achieve the observed peculiar velocity, with either a large amount of mass ($\sim 11M_{\odot}$) being lost in the explosion, or, more probably, the system being subject to an asymmetric kick. In the case of a pure Blaauw kick, $\sim 1M_{\odot}$ must have been transferred from the donor to the black hole since the onset of mass transfer, implying an initial black hole mass of $\sim 9M_{\odot}$ with a donor mass of $\sim 2M_{\odot}$ prior to the onset of mass transfer.

ACKNOWLEDGMENTS

J.C.A.M.-J. is a Jansky Fellow of the National Radio Astronomy Observatory. E.G. is supported through Chandra Postdoctoral Fellowship grant number PF5-60037, issued by the Chandra X-Ray Center, which is operated by the Smithsonian Astrophysical Observatory for NASA under contract NAS8-03060. The VLA and VLBA are facilities of the National Radio Astronomy Observatory which is operated by Associated Universities, Inc., under cooperative agreement with the National Science Foundation. The European VLBI Network is a joint facility of European, Chinese, South African and other radio astronomy institutes funded by their national research councils. ParselTongue was developed in the context of the ALBUS project, which has benefited from research funding from the European Community's sixth Framework Programme under RadioNet R113CT 2003 5058187. This research has made use of NASA's Astrophysics Data System.

REFERENCES

- Binney J., Merrifield M., 1998, *Galactic Astronomy* (Princeton: Princeton University Press)
- Blaauw A., 1961, *Bull. Astron. Inst. Netherlands*, 15, 265
- Bradshaw C. F., Fomalont E. B., Geldzahler B. J., 1999, *ApJ*, 512, L121
- Brandt N., Podsiadlowski P., 1995, *MNRAS*, 274, 461
- Brandt W. N., Podsiadlowski Ph., Sigurdsson S., 1995, *MNRAS*, 277, L35
- Carlberg R. G., Innanen K. A., 1987, *AJ*, 94, 666
- Casares J., Charles P. A., 1994, *MNRAS*, 271, L5
- Casares J., Charles P. A., Naylor T., Pavlenko E. P., 1993, *MNRAS*, 265, 834
- Cowley A. P., Crampton D., 1975, *ApJ*, 201, L65
- Dehnen W., Binney J. J., 1998, *MNRAS*, 298, 387
- Dhawan V., Mirabel I. F., Ribó M., Rodrigues I., 2007, *ApJ*, 668, 430
- Dhawan V., Mioduszewski A. J., Rupen M. P., 2006, in Belloni T., ed., *Proceedings of the "VI Microquasar Workshop: Microquasars and Beyond"*, PoS: Trieste, 52
- Edvardsson B., Andersen J., Gustafsson B., Lambert D. L., Nissen P. E., Tomkin J., 1993, *A&A*, 275, 101
- Flynn C., Sommer-Larsen J., Christensen P. R., 1996, *MNRAS*, 281, 1027
- Fragos T., Willems B., Kalogera V., Ivanova N., Rockefeller G., Fryer C. L., Young P. A., 2008, arXiv:0809.1588
- Fryer C. L., Kalogera V., 2001, *ApJ*, 554, 548
- Greiner J., Cuby J. G., McCaughrean M. J., 2001, *Nature*, 414, 522
- Greisen E. W., 2003, in *Information Handling in Astronomy: Historical Vistas*, ed. A. Heck (Dordrecht: Kluwer), 109
- Gualandris A., Colpi M., Portegies Zwart S., Possenti A., 2005, *ApJ*, 618, 845
- Han X., Hjellming R. M., 1992, *ApJ*, 400, 304
- Hansen B. M. S., Phinney E. S., 1997, *MNRAS*, 291, 569
- Herrero A., Kudritzki R. P., Gabler R., Vilchez J. M., Gabler A., 1995, *A&A*, 297, 556
- van den Heuvel E. P. J., van Paradijs J., 1997, *ApJ*, 483, 399
- van den Heuvel E. P. J., Portegies Zwart S. F., Bhattacharya D., Kaper L., 2000, *A&A*, 364, 563
- Johnson D. R. H., Soderblom D. R., 1987, *AJ*, 93, 864
- Johnston K. V., Spergel D. N., Hernquist L., 1995, *ApJ*, 451, 598
- Jonker P. G., Nelemans G., 2004, *MNRAS*, 354, 355
- King A. R., 1993, *MNRAS*, 260, L5
- Kuijken K., Gilmore G., 1989, *MNRAS*, 239, 571
- Lai D., Chernoff D. F., Cordes J. M., 2001, *ApJ*, 549, 1111
- Lyne A. G., Lorimer D. R., 1994, *Nature*, 369, 127
- Mignard F., 2000, *A&A*, 354, 522
- Miller-Jones J. C. A., Gallo E., Rupen M. P., Mioduszewski A. J., Briske W., Fender R. P., Jonker P. G., Maccarone T. J., 2008, *MNRAS*, 388, 1751
- Mirabel I. F., 2008, arXiv:0805.2378
- Mirabel I. F., Rodrigues I., 2003a, *Science*, 300, 1119
- Mirabel I. F., Rodrigues I., 2003b, *A&A*, 398, L25
- Mirabel I. F., Dhawan V., Mignani R. P., Rodrigues I., Guglielmetti F., 2001, *Nature*, 413, 139
- Mirabel I. F., Mignani R., Rodrigues I., Combi J. A., Rodríguez, L. F., Guglielmetti F., 2002, *A&A*, 395, 595
- Nelemans G., Tauris T. M., van den Heuvel E. P. J., 1999, *A&A*, 352, L87
- de Oliveira M. R., Fausti A., Bica E., Dottori H., 2002, *A&A*, 390, 103
- Orosz J. A., 2003, in van der Hucht K., Herrero A., Esteban C., eds, *Proc. IAU Symp. 212, A Massive Star Odyssey: From Main Sequence to Supernova*. Astron. Soc. Pac., San Francisco, p. 365
- Paczyński B., 1990, *ApJ*, 348, 485
- Podsiadlowski Ph., Rappaport S., Han Z., 2003, *MNRAS*, 341, 385
- Portegies Zwart S. F., Yungelson L. R., 1998, *A&A*, 332, 173
- Press W. H., Teukolsky S. A., Vetterling W. T., Flannery B. P., 1992, *Numerical Recipes in C: The Art of Scientific Computing* (Ed. 2; Cambridge: Cambridge University Press)
- Reid M. J., 1993, *ARA&A*, 31, 345
- Reid M. J., Brunthaler A., 2004, *ApJ*, 616, 872
- Ribó M., Paredes J. M., Romero G. E., Benaglia P., Martí J., Fors O., García-Sánchez J., 2002, *A&A*, 384, 954
- Sanwal D., Robinson E. L., Zhang E., Colome C., Harvey P. M., Ramseyer T. F., Hellier C., Wood J. H., 1996, *ApJ*,

460, 437

Shahbaz T., Ringwald F. A., Bunn J. C., Naylor T., Charles P. A., Casares J., 1994, *MNRAS*, 271, L10

White N. E., van Paradijs J., 1996, *ApJ*, 473, L25

Wielen R., 1977, *A&A*, 60, 263

Willems B., Henninger M., Levin T., Ivanova N., Kalogera V., McGhee K., Timmes F. X., Fryer C. L., 2005, *ApJ*, 625, 324

Wolfire M. G., McKee C. F., Hollenbach D., Tielens A. G. G. M., 1995, *ApJ*, 453, 673